

Synthesis of Neocannabinoids Using Controlled Friedel-Crafts Reactions

Alexandra M. Millimaci, Richard V. Trilles, James McNeely, Lauren E. Brown, Aaron B. Beeler,* and John A. Porco, Jr.*

Department of Chemistry, Boston University, Boston, Massachusetts 02215, United States

ABSTRACT: A simple, one-step transformation to produce 8,9-dihydrocannabidiol (H₂CBD) and related “neocannabinoids” via controlled Friedel-Crafts reactions is reported. Experimental and computational studies probing the mechanism of neocannabinoid synthesis from cyclic allylic alcohol and substituted resorcinol reaction partners provide understanding of the kinetic and thermodynamic factors driving regioselectivity for the reaction. Herein, we present a reaction scope for neocannabinoid synthesis including the production of both normal and abnormal isomers under both kinetic and thermodynamic control. Discovery and optimization of this one-step protocol between various allylic alcohols and resorcinol derivatives is discussed and supported with density-functional theory (DFT) calculations.

INTRODUCTION

Cannabidiol (CBD) **1** (Figure 1) was discovered in 1940 and is one of more than 100 identified cannabinoids in cannabis plants; together, CBD and tetrahydrocannabinol (THC) **2**, account for almost half of the plant's extract.^{1,2} Although CBD has shown promise in therapeutic uses for Alzheimer's disease,³ Parkinson's disease,³ and cancer,³ its psychoactive effects and propensity for intramolecular cyclization to generate the DEA Schedule I-controlled substance THC (**2**) have limited its utility and potential.^{4,5} Furthermore, marketing of CBD for consumption carries the risk of illicit use in the production of THC analogues in analogy to challenges associated with pseudoephedrine-to-methamphetamine.^{6,7} These concerns have highlighted the potential of the synthetic cannabinoid 8,9-dihydrocannabidiol (H₂CBD) **3** to abrogate these concerns due to saturation of the exocyclic isoprene moiety, thereby preventing electrophilic cyclization to THC.⁶ Thus, H₂CBD poses no legal issues as it is fully synthetic, can be scaled up from readily available starting materials that do not require cultivation of cannabis or hemp, and poses no concern for the generation of THC. Such molecules could provide a path toward cannabinoid-based therapeutics without psychotropic effects to prevent drug abuse liabilities.

In parallel studies involving CBD and abnormal cannabidiol **4** (Abn-CBD) it was found that their affinities for CB₁ and CB₂ receptors were substantially different.^{8,9} It was then discovered that Abn-CBD and synthetic analogs (e.g. **5**, O-1602) have binding affinities to the orphaned cannabinoid receptors, GPR18 and GPR55, two receptors which are responsible for effects of cannabinoids independent of CB₁ and CB₂.⁹ Abnormal CBD **4** is a CBD regioisomer in which the terpene subunit is positioned *ortho* to the *n*-pentyl substituent (vs. the *para* relationship present in “normal” CBD **1**), a structural difference for binding to other targets in future analogs. Further structure-activity relationship (SAR) studies show that the substitution of the alkyl chain from Abn-CBD, the relative position of aromatic groups, and sites with the ability to form hydrogen-bonds are important for binding to GPR18 and GPR55.^{9,10} These findings suggest that synthetic investigations towards new, unnatural cannabinoid derivatives and isomers (herein referred to as “neocannabinoids”) including abnormal H₂CBD **6** can greatly benefit therapeutic applications.^{11,12,13}

A number of routes for the chemical synthesis of CBD and related molecules have been devised (Scheme 1).^{14–17} The most efficient approach leverages Friedel-Crafts alkylation of olivetol **7** and chiral allylic alcohols such as menthadienol **8** under mild acidic conditions affording CBD through an S_N1' mechanism. (Scheme 1A).^{15,18} These reactions typically deliver exclusive diastereoselectivity wherein the olivetol substituent favors a *trans* orientation relative to the isopropyl group. Notably these reactions generally lack regioselectivity between the (“abnormal”) **4** and (“normal”) **1** isomers. Production of the generally undesired abnormal CBD isomer is often a complication in the synthetic production of CBD via the Friedel-Crafts route and can be further complicated by unwanted cycloetherification when using Brønsted acid catalysis. To address this issue, Baek and coworkers reported the synthesis of CBD **1** in 56% isolated yield along with 14% abnormal CBD isomer **4** using BF₃•OEt₂ on alumina (Al₂O₃) as Lewis acid promoter.^{15,19} Other modes of

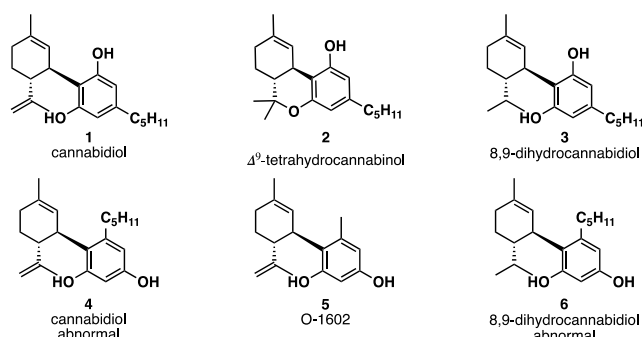
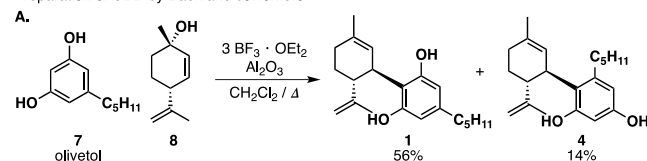


Figure 1. Natural and synthetic cannabinoids.

Scheme 1. Synthesis of CBD isomers and dihydro-CBD regioisomers

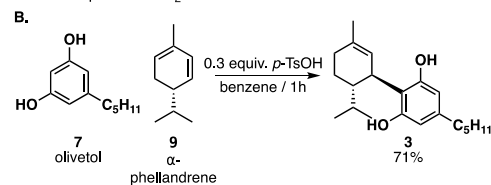
Olivetol-based synthesis of CBD

Preparation of CBD by Baek and coworkers

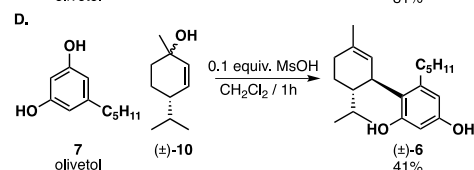
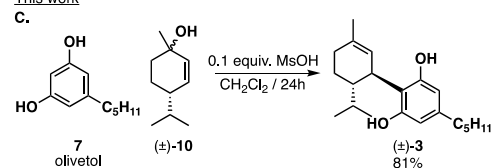


Relevant analog synthesis

Mascal Preparation of H₂CBD



This work



entry to synthetic CBD include the use of olivetol derivatives to control the site of reaction by removable “blocking group” strategies (*e.g.* ester or halogens), thereby inhibiting abnormal product formation.¹⁵ This method, which mimics the biosynthesis of CBD, generally involves multiple synthetic steps to access CBD in good yields.⁵

The challenge in controlling regioselectivity of CBD synthesis without cyclization to THC birthed the expansion into the synthesis of relevant analogs. The racemic, reduced version of CBD (H₂CBD) **3** displays similar pharmacological properties to CBD and does not require chiral pool starting materials making it a promising synthetic target. Importantly, synthetic generation of H₂CBD provides room for reaction manipulation and optimization to control regioselectivity without the concern of unintended THC production. This prompted our efforts to develop a better understanding of the kinetic and thermodynamic factors that dictate regioselectivity in this reaction.

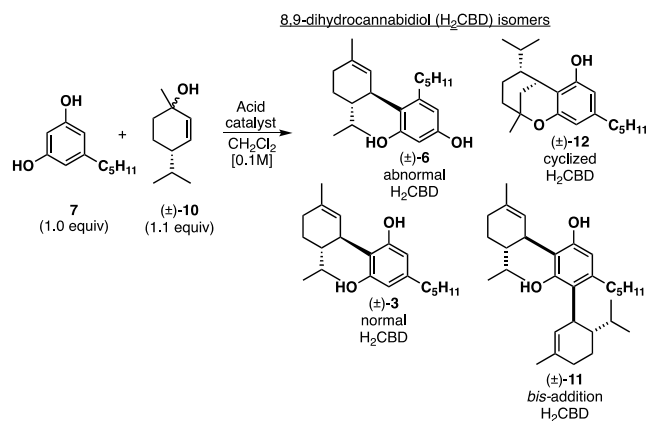
Herein, we describe our efforts toward an efficient and regioselective synthesis of normal and abnormal neocannabinoids. In this study, we confirmed that regioselectivity is largely controlled by both kinetic and thermodynamic considerations. Our findings were aligned with computational studies, thereby providing a model for a range of reaction partners and product distributions.

RESULTS AND DISCUSSION

We began our investigation by screening numerous Lewis and Brønsted acids to initiate allylic cation chemistry by mimicking the effects of BF₃·OEt₂ as reported in the literature.^{20–22} Previously, Mascal and coworkers obtained normal CBD **3** in 71% yield by *para*-toluenesulfonic acid (*p*-TsOH) acid-catalyzed addition to α-phellandrene **9** (Scheme 1B).^{6,15} In an effort

to match this efficiency, we considered the well-established Friedel-Crafts alkylation/cationic intermediate pathway using olivetol **7** and allylic alcohol **10** to access H₂CBD isomers **3** and **6** (Scheme 1C–D). Our catalyst scope included various Lewis acids including Sc(III)-, La(III)-, Eu(III)-, Yb(III)- triflates, *p*-TsOH and MsOH, as well as combinations of both Lewis and Brønsted acids. Metal triflates were tested over multiple time points with varying catalyst loadings and temperatures. All conditions screened provided a mixture of normal H₂CBD **3** and abnormal H₂CBD **6** (Table 1); in many cases, the *bis*-addition product **11** was also observed; reactions conducted at higher temperatures (40 °C) provided only cyclized products.^{23–25} La(III)- and Yb(III)- triflates provided the highest conversion to H₂CBD **3** after 24 h, but also led to increased production of *bis*-addition product **11** which was ultimately a significant drawback for use of metal triflates. *p*-TsOH and MsOH both performed well in the reaction and optimally in CH₂Cl₂, although use of *p*-TsOH led to solubility issues. Thus, optimal reaction conditions were found using MsOH as catalyst. The friendliness of MsOH as a liquid with low corrosivity and toxicity in comparison to the other Brønsted acids made it very easy to work with.²⁶

Table 1. Acid screening scope for Friedel-Crafts reactions



En-try	Acid	Amt.	Time (h)	Conver-sion ^a	(±)- 6 ^b	(±)- 3 ^b
1	La(OTf) ₃	20 mol%	1	35%	10%	25%
2			24	78%	4%	52%
3	Yb(OTf) ₃	20 mol%	1	35%	10%	25%
4			24	75%	9%	47%
5	MsOH	10 mol%	1	90%	41% ^b	39%
6			24	99%	0%	81% ^b
7	<i>p</i> -TsOH	10 mol%	1	78%	30%	36%
8			24	91%	8%	63%

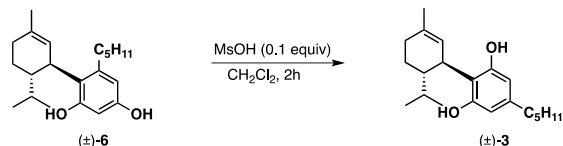
^a Conversion measured by ¹H NMR analysis.

^b Isolated yield after silica gel chromatography.

The MsOH-catalyzed reaction was optimized by evaluating catalyst loading, temperature, and time. In these studies, we found that initially the reaction generated roughly a 1:1 ratio of normal H₂CBD **3** to abnormal derivative **6** as well as *bis*-addition product **11** as a side product. However, we observed greater

conversion to H₂CBD as determined by ¹H NMR analysis at a 24 h reaction time. Allowing the reaction to proceed beyond 24 h increased the amount of cycloetherification product **12**; accordingly, optimal reaction conditions to generate H₂CBD were 0.1 equiv. of MsOH at room temperature for 24h (**Table 1**, entry 6). However, we believed that the apparent conversion from abnormal to normal isomers suggested that production of **6** could be a kinetic process and by terminating the reaction at an earlier timepoint, we could increase selectivity. Indeed, we were able to obtain abnormal H₂CBD **6** (rr = 1:1) in 41% isolated yield after 1 h reaction time (**Table 1**, entry 5), in contrast to an 81% isolated yield of normal H₂CBD **3** after 24 h.

Table 2. Equilibration of abnormal to normal H₂CBD by *in situ* ¹H NMR analysis



time (h)	(±)- 6	(±)- 3	byproducts (±)- 11 and (±)- 12
1	40%	60%	0
2	10%	90%	0
6	2%	74%	24%
24	0%	50%	50%

We next tested the abnormal to normal equilibration hypothesis with a time study by treating pure abnormal isomer **6** with catalytic amounts of MsOH in CH₂Cl₂. We observed that the abnormal product does in fact equilibrate to the normal product **3** in as quickly as 1 h, with full consumption of **6** observed over a longer time period albeit with concomitant emergence of by-products **11** and **12** (**Table 2**). Further screening was also conducted with *p*-TsOH and camphorsulfonic acid (CSA) as catalysts (*not shown*), but these acids exhibited poor solubility in CH₂Cl₂ and produced greater amounts of side products. Previous work by Crombie and coworkers showed that reactions of olivetol with electrophiles such as (+)-*trans*-car-2-ene epoxide²⁵ and **9**²⁷ in the presence of *p*-TsOH also afforded both abnormal and normal cannabinoids at early timepoints, with an “interconversion” of abnormal to normal occurring with elevated temperatures.²⁸ Consistent with our findings, it was noted that in this process the presumably kinetically favored abnormal cannabinoid transforms to the presumed more thermodynamically stable normal cannabinoid.²⁷

Further probing of a potential dissociative equilibration process was performed in a crossover experiment to refine mechanistic understanding. The experiment shown in **Scheme 2** was designed using two different abnormal cannabinoids, **6** and **13**, which were treated under the same acidic conditions. Abnormal cannabinoid isomer **13** was prepared using divarinol and 1-methylcyclohex-2-en-1-ol as reaction partners. In this experiment, we expected equilibration from abnormal to normal cannabinoid *e.g.* **6** to **3** and **13** to **14**, as well as crossover products **15** and **16**, assuming that equilibration proceeds by disassociation to regenerate the allylic cation and resorcinol partner (**Scheme 3**).

Scheme 2. Crossover experiment between abnormal cannabinoids **6 and **13****

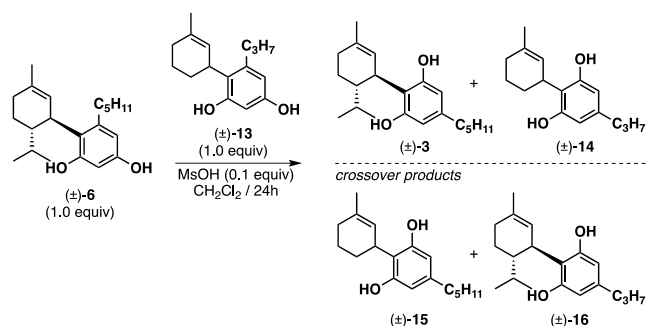
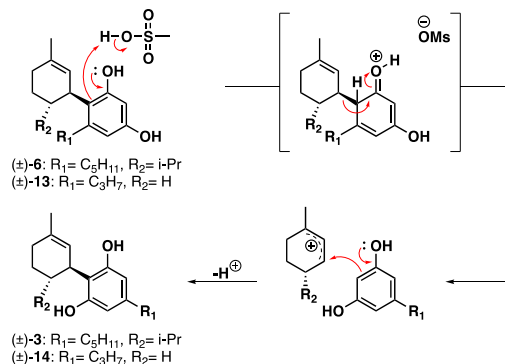


Table 3. Tracking formation of crossover products during equilibration by HPLC-ELSD/MS

time (h)	area % (±)- 15 and (±)- 16
1	trace
2	trace
24	26%

Using a combination of *in situ* ¹H NMR and LC/MS analysis, we monitored the ratios of the pure abnormal cannabinoids **6/13**, their corresponding normal isomers **3/14**, and expected crossover products **15/16** (**Table 3**). As expected, we observed products **3** and **14** after 1 h, with only trace amounts of **15** and **16** detected; after 24 h, we obtained a considerable amount (26%) of crossover products.²⁹ Overall, this data confirmed that the generation of **6** from **3** (*cf.* **Table 2**) likely proceeds *via* an intermolecular retro-Friedel Crafts/Friedel-Crafts process³⁰ and not an intramolecular rearrangement.

Scheme 3. Proposed mechanism for equilibration of abnormal to normal neocannabinoids **6 and **13** to **3** and **14****

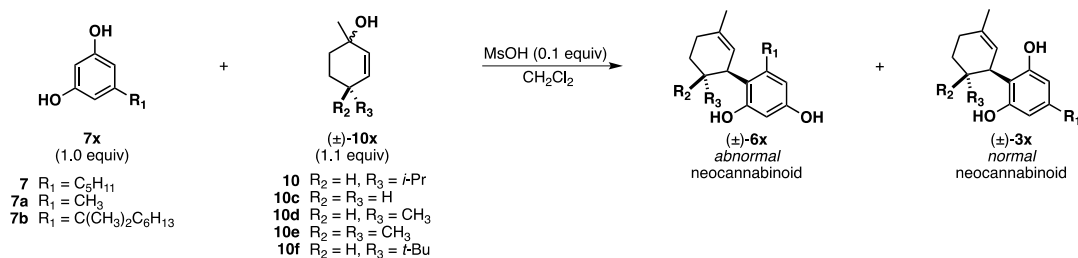


We next sought to prepare a small library of allylic alcohols for neocannabinoid synthesis. We envisioned a scope of allylic alcohols varying in substituents at the 4-position to determine the steric effects of normal *vs.* abnormal addition in terms of both kinetic and thermodynamic control. Five reagents (**10-10f**) were chosen to represent a gradual increase in sterics progressing from no substituents (**10c**) to the bulky *tert*-butyl substituted partner (**10f**). Likewise, selection of the resorcinol reagent also varied in both sterics and alkyl chain length. We chose orcinol (**7a**), olivetol (**7**), and 5-(1,1-dimethylheptyl) resorcinol (**7b**) as three reaction partners as shown in **Table 4**.

For all reagent pairings, we tracked the ratio of isomers generated at both 1 and 24 h by both HPLC and ¹H NMR analyses. We found that in almost all cases employing orcinol **7a** (Table 4, entries 1-4), the abnormal neocannabinoid **6ac-6a** was enriched within the first hour. The *tert*-butyl allylic alcohol (**10f**, Table 4, entry 5) was the only example where the normal neocannabinoid (**3af**) was the major product at the 1 h timepoint. The kinetic preference for the abnormal isomers can also be attributed to favorable electrostatics (Löwdin charges) between the *ortho* (relative to the resorcinol alkyl chain) carbons and the cationic partner as compared to the *para* carbons (see Figure S1 in the Supporting Information). Overall, we observed that the ratio of normal:abnormal (**3ac-3af**:**6ac-6af**) increases over time, consistent with our observation of a thermodynamic equilibration process. In order to rationalize these outcomes, the systems were studied computationally (Orca, r²SCAN-3C/CPCM(CH₂Cl₂))³¹⁻³⁵ to understand the kinetic and

thermodynamic factors driving the 1 h/24 h ratios observed (Table 4 and Supporting Information). Indeed, our calculations generally support the premise that with increasing bulk at the 4-position of the allylic alcohol partner, the normal product is increasingly thermodynamically favored (ΔG in Table 4), a likely consequence of the added steric strain introduced between the R₂/R₃ substituents and the R₁ sidechain. The computations suggest a kinetic preference for the abnormal isomer in **3(6)ac-3(6)ae** and **3(6)af** with k^3/k^6 ratios less than 1. Even for **3/6a**, the observed ratio of 1.2 is close to unity. These thermodynamic and reactivity trends also held for reactions with the same set of allylic alcohols and olivetol **7** (Table 4, entries 6-10). It should be noted that the key difference in orcinol vs. olivetol is the alkyl chain (pentyl vs. methyl group); this change did impact the results for obtaining high ratios of normal to abnormal neocannabinoids.

Table 4. Kinetic vs. thermodynamic study of various neocannabinoids with experimental selectivity ratios and DFT-calculated energies



Entry	Resorcinol 7	Allylic alcohol 10	(r.r.), 1 h (3:6) ^a	(r.r.), 24 h (3:6) ^a	Isolated product (±)- 3	% Yield isolated (±)- 3 , 24 h	Computational results	
							k^3/k^6 ^b	ΔG (kcal/mol) ^c
1	7a	10c	(1:3)	(1:1)	3ac	9%	0.48	1.3
2	7a	10d	(2:5)	(3:4)	3ad	37%	0.24	1.7
3	7a	10e	(1:10)	(3:10)	3ae	16%	0.48	5.9
4	7a	10	(2:3)	(11:1)	3a	47%	1.20	4.8
5	7a	10f	(5:1)	(9:1)	3af	51%	0.34	4.0
6	7	10c	(7:10)	(1:1)	3c	43%	0.67	1.0
7	7	10d	(1:1)	(5:1)	3d	56%	0.85	4.0
8	7	10e	(1:4)	(1:3)	3e	18%	0.51	2.1
9	7	10	(11:10)	(1:0)	3	88%	0.49	1.7
10	7	10f	(27:1)	(25:1)	3f	75%	2.34	1.7
11	7b	10c	(1:0)	(1:0)	3bc	98%	4.52	7.3
12	7b	10d	(1:0)	(1:0)	3bd	98%	8.80	9.3
13	7b	10e	(1:0)	(1:0)	3be	72%	206.01	11.4
14	7b	10	(1:0)	(1:0)	3b	79%	49.72	10.8
15	7b	10f	(1:0)	(1:0)	3bf	56%	117.65	11.9

^a Ratio determined by HPLC/ELSD/MS and ¹H NMR analysis.

^b $k^3/k^6 = e^{\Delta\Delta G/kT}$, where $\Delta\Delta G = G(6x^\ddagger) - G(3x^\ddagger)$, T = 298.15 K, and G(3/6x[‡]) is the Boltzmann-averaged free energy.

^c $\Delta G = G(6x) - G(3x)$, where G(3/6x) is the Boltzmann-averaged free energy.

Table 5. Optimized syntheses of abnormal neocannabinoid derivatives

7 $R_1 = C_6H_{11}$
7a $R_1 = CH_3$
7b $R_1 = C(CH_3)_2C_6H_{13}$

10 $R_2 = H, R_3 = nPr$
10c $R_2 = R_3 = H$
10d $R_2 = H, R_3 = CH_3$
10e $R_2 = R_3 = CH_3$
10f $R_2 = H, R_3 = tBu$

Entry	Resorcinol 7	Allylic alcohol 10	Isolated product (\pm)- 6	% Isolated yield (\pm)- 6
1	7a	10c	6ac	35%
2	7a	10d	6ad	50%
3	7a	10e	6ae	33%
4	7a	10	6a	40%
5	7	10c	6c	50%
6	7	10d	6d	37%
7	7	10e	6e	24%
8	7	10	6	41%

We next hypothesized that an increase in steric bulk on the resorcinol alkyl chain could further drive initial formation of the normal neocannabinoid isomer.²⁹ This hypothesis led us to evaluate the bulky 5-(1,1-dimethylheptyl) resorcinol partner **7b**. Using this resorcinol partner, we observed formation

of the normal neocannabinoid as the major isomer at 1 h with all allylic alcohols employed which we posited was due to increased steric strain imposed by the dimethyl heptyl chain (**3bc-3bf**). DFT calculations also confirmed that the normal isomers were significantly more stable as reaction products and were also kinetically preferred.

Overall, the experimental and computational findings shown in **Table 4** support a mechanism that initially produces the abnormal neocannabinoid when there is less steric bulk surrounding the cation intermediate and the normal neocannabinoid in cases of greater steric bulk. This mechanistic correlation can be visualized by the select examples shown in **Figure 2** outlining the computed differences in Gibbs free energy of the corresponding abnormal and normal isomer transition states. We also noticed that many transition states leading to both normal and abnormal isomers displayed stabilization imparted by C-H- π interactions³⁶ (see Supporting Information). **Figure 3** shows examples of global minimum transition states highlighting these interactions enroute to normal H₂CBD isomer **3** and abnormal isomer **6**. As shown in **Figure 2**, the difference in the alkyl chain of products **3ad** and **6ad** vs. **3d** and **6d** show that the energy needed to kinetically form abnormal product **6ad** is preferred in comparison to the energy needed to form abnormal isomer **6d**. By leveraging this mechanism and terminating the reaction at different timepoints, we can favor production of either normal or abnormal neocannabinoids based on steric considerations. As previously described, efficient synthesis of abnormal analogues could be a valuable asset in cannabinoid therapeutics; **Table 5** highlights examples of abnormal isomers accessed in moderate yields by terminating the reaction at a 1 h timepoint.

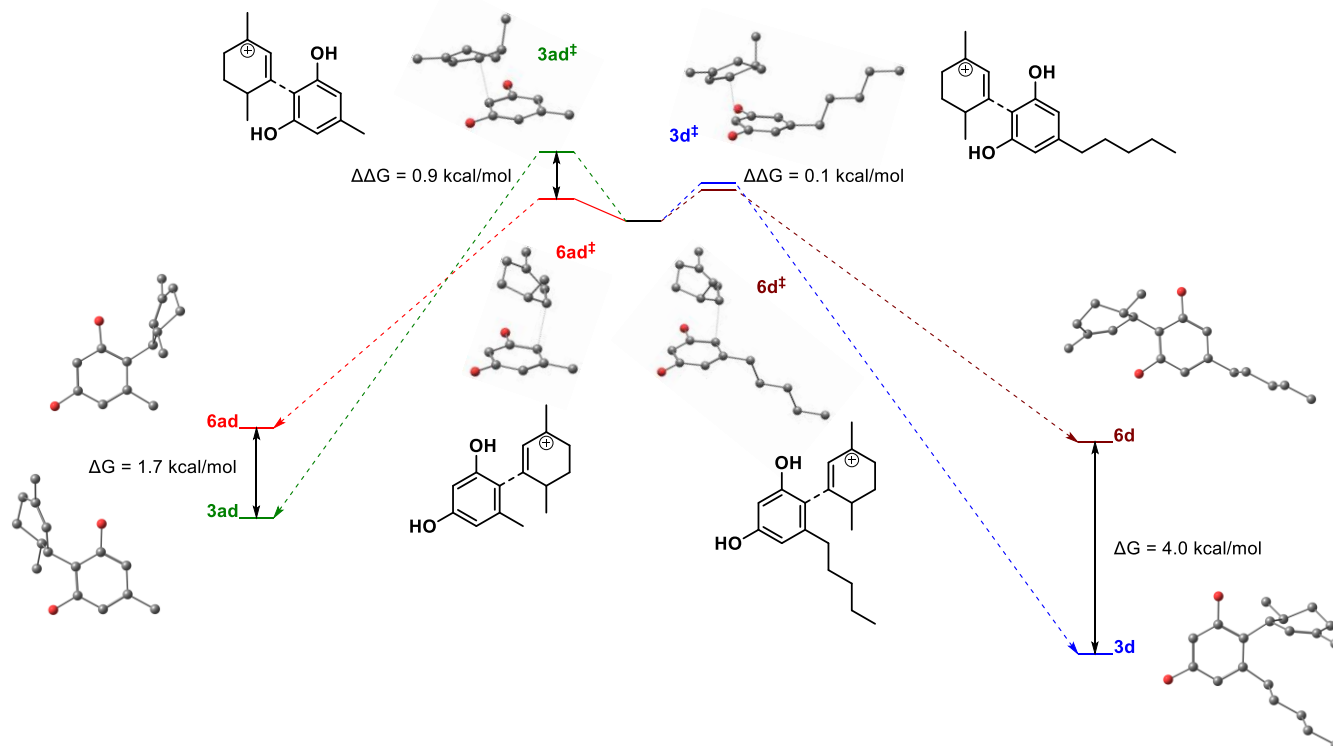


Figure 2. Qualitative energy diagrams for neocannabinoid isomers **3ad**, **6ad**, **3d**, and **6d** with the corresponding 3D models. The positions of isomer pairs on the y-axis are a guide for the eyes only and are not meant to represent absolute energies.

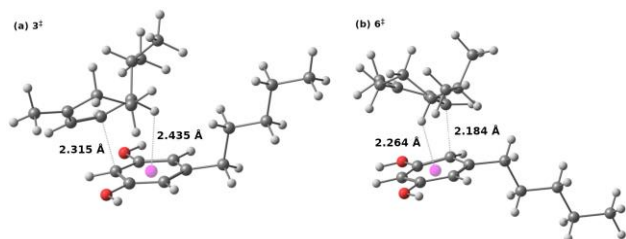
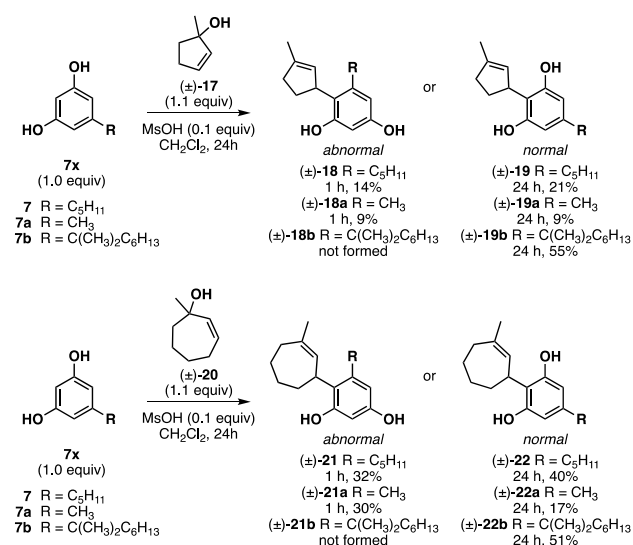


Figure 3. Global minimum transition state structures for normal (**a**, **3[‡]**) and abnormal (**b**, **6[‡]**) isomers highlighting the stabilization imparted by C-H π interactions. The pink sphere is the center of the resorcinol aryl ring.

As a final study, we sought to test whether the condition-dependent regioselective reactions could also be applied to access neocannabinoids with alternative, unnatural ring sizes for the terpenoid fragment. Accordingly, we synthesized both 5- and 7-member cyclic allylic alcohols **17** and **20**, respectively, and subjected them to the general reaction conditions shown in **Scheme 4**. These reactions were found to tolerate each ring size and both abnormal and normal neocannabinoids were generated and isolated in each case. When tracking these reactions, we again observed, in cases with orcinol and olivetol, that abnormal products (**18**, **19**, **20**, **21**) were produced in competition with the normal isomers (**18a**, **19a**, **21a**, **22a**) and over time produced more normal isomer due to product equilibration. Use of 5-(1,1-dimethylheptyl) resorcinol as reaction partner again supported the idea that steric bulk inhibits formation of abnormal products (**19b**, **22b**) where only the normal neocannabinoid product was observed with use of both 5- and 7-member cyclic allylic alcohols.

Scheme 4. Neocannabinoid synthesis from alternate cyclic allylic alcohols



CONCLUSIONS

Herein, we report the synthesis of diverse neocannabinoids using controlled Friedel-Crafts reactions to control construction of either the abnormal or normal isomer. We have demonstrated the scope and limitations of this process over 35 examples to produce synthetic unnatural analogs of both normal and abnormal cannabidiol (CBD). Improved understanding of the kinetic and thermodynamic properties for the reaction can be leveraged in the future towards predictive neocannabinoid

synthesis. Moreover, our ongoing and future studies will continue to investigate the power of neocannabinoids as therapeutics and in targeted medicinal chemistry applications which will be the subject of future publications.

ASSOCIATED CONTENT

Supporting Information

The Supporting Information is available free of charge on the ACS Publications website.

Experimental procedures, analytical data, ¹H and ¹³C NMR spectra of all newly synthesized compounds, and DFT calculation details (PDF).

AUTHOR INFORMATION

Corresponding Authors

*E-mail: porco@bu.edu (J.A.P, Jr.)

E-mail: beelera@bu.edu (A.B.B)

Author Contributions

The manuscript was written through contributions of all authors. All authors have given approval to the final version of the manuscript.

Funding Sources

This research was funded by NIH GM118173.

Notes

The authors declare the following competing financial interest(s): J.A.P, Jr. A.B, A. M., R.T., J.M., and L.E.B are inventors on a provisional patent application describing the synthesis of neocannabinoid isomers.

ACKNOWLEDGMENTS

The authors thank Dr. Norman Lee of the Boston University Chemical Instrumentation Center for HRMS data and analyses. We thank CBDQure Inc. for funding the initial phases of the project and the National Institutes of Health (NIH) (R35 GM 118173) for additional financial support. We also thank Nick Wangtz (Shanghai Xishite Biosciences Co., Ltd.) for a generous donation of divarinol. We also thank the National Science Foundation (NSF) for support of NMR (CHE-0619339) and MS (CHE-0443618) facilities at Boston University.

ABBREVIATIONS

CBD, cannabidiol; THC, tetrahydrocannabinol; H₂CBD, 8,9-dihydrocannabidiol; Abn-CBD, abnormal cannabidiol, DFT density-functional theory; GPR, G-protein coupled receptor, NMR; nuclear magnetic resonance; HPLC, high-performance liquid chromatography.

REFERENCES

- (1) Adams, R.; Hunt, M.; Clark, J. H.; Clark1, J. H.; Loewe, D. S. *Yol. 62 Structure of Cannabidiol, a Product Isolated from the Marijuana Extract of Minnesota Wild Hemp. I.* <https://pubs.acs.org/sharingguidelines>.
- (2) Atalay, S.; Jarocka-karpowicz, I.; Skrzydlewska, E. Antioxidative and Anti-Inflammatory Properties of Cannabidiol. *Antioxidants*. MDPI January 1, 2020. <https://doi.org/10.3390/antiox9010021>.
- (3) Pisanti, S.; Malfitano, A. M.; Ciaglia, E.; Lamberti, A.; Ranieri, R.; Cuomo, G.; Abate, M.; Faggiana, G.; Proto, M. C.; Fiore, D.; Laezza, C.; Bifulco, M. Cannabidiol: State of the Art and New Challenges for Therapeutic Applications. *Pharmacology and Therapeutics*. Elsevier Inc. July 1, 2017, pp 133–150. <https://doi.org/10.1016/j.pharmthera.2017.02.041>.
- (4) Ben-Shabat, S.; Hanuš, L. O.; Katzavian, G.; Gallily, R. New Cannabidiol Derivatives: Synthesis, Binding to Cannabinoid Receptor, and Evaluation of Their Antiinflammatory Activity. *J Med Chem* **2006**, *49* (3), 1113–1117. <https://doi.org/10.1021/jm050709m>.
- (5) Nelson, K. M.; Bisson, J.; Singh, G.; Graham, J. G.; Chen, S. N.; Friesen, J. B.; Dahlin, J. L.; Niemitz, M.; Walters, M. A.; Pauli, G. F. The Essential Medicinal Chemistry of Cannabidiol (CBD). *Journal of Medicinal Chemistry*. American Chemical Society November 12, 2020, pp 12137–12155. <https://doi.org/10.1021/acs.jmedchem.0c00724>.
- (6) Mascal, M.; Hafezi, N.; Wang, D.; Hu, Y.; Serra, G.; Dallas, M. L.; Spencer, J. P. E. Synthetic, Non-Intoxicating 8,9-Dihydrocannabidiol for the Mitigation of Seizures. *Sci Rep* **2019**, *9* (1). <https://doi.org/10.1038/s41598-019-44056-y>.
- (7) Bloemendal, V. R. L. J.; van Hest, J. C. M.; Rutjes, F. P. J. T. Synthetic Pathways to Tetrahydrocannabinol (THC): An Overview. *Organic and Biomolecular Chemistry*. Royal Society of Chemistry May 7, 2020, pp 3203–3215. <https://doi.org/10.1039/d0ob00464b>.
- (8) Leite, R.; Carlini, E. A.; Lander, N.; Mechoulam, R. Anti-convulsant Effects of the (-) and (+) Isomers of Cannabidiol and Their Dimethylheptyl Homologs. *Pharmacology* **1982**, *24* (3), 141–146. <https://doi.org/10.1159/000137588>.
- (9) C. Ashton, J. The Atypical Cannabinoid O-1602: Targets, Actions, and the Central Nervous System. *Cent Nerv Syst Agents Med Chem* **2012**, *12* (3), 233–239. <https://doi.org/10.2174/187152412802430156>.
- (10) Johns, D. G.; Behm, D. J.; Walker, D. J.; Ao, Z.; Shapland, E. M.; Daniels, D. A.; Riddick, M.; Dowell, S.; Staton, P. C.; Green, P.; Shabon, U.; Bao, W.; Aiyar, N.; Yue, T. L.; Brown, A. J.; Morrison, A. D.; Douglas, S. A. The Novel Endocannabinoid Receptor GPR55 Is Activated by Atypical Cannabinoids but Does Not Mediate Their Vasodilator Effects. *Br J Pharmacol* **2007**, *152* (5), 825–831. <https://doi.org/10.1038/sj.bjp.0707419>.
- (11) Hanuš, L. O.; Meyer, S. M.; Muñoz, E.; Tagliatalata-Scafati, O.; Appendino, G. Phytocannabinoids: A Unified Critical Inventory. *Natural Product Reports*. Royal Society of Chemistry December 1, 2016, pp 1357–1392. <https://doi.org/10.1039/c6np00074f>.
- (12) Jentsch, N. G.; Zhang, X.; Magolan, J. Efficient Synthesis of Cannabigerol, Grifolin, and Piperogalin via Alumina-Promoted Allylation. *J Nat Prod* **2020**, *83* (9), 2587–2591. <https://doi.org/10.1021/acs.jnatprod.0c00131>.
- (13) Kearney, S.; Gangano, A.; Navaratne, P.; Barrus, D.; Rehrauer, K.; Reid, T.-E.; Roitberg, A.; Ghiviriga, I.; Cunningham, C.; Gamage, T.; Grenning, A. Axially Chiral Cannabinoids: Design, Synthesis, and Cannabinoid Receptor Affinity. *ChemRxiv*. *This content is a preprint and has not been peer-reviewed.* **2023**.
- (14) Lago-Fernandez, A.; Redondo, V.; Hernandez-Folgado, L.; Figuerola-Asencio, L.; Jagerovic, N. New Methods for the Synthesis of Cannabidiol Derivatives. In *Methods in Enzymology*; Academic Press Inc., 2017; Vol. 593, pp 237–257. <https://doi.org/10.1016/bs.mie.2017.05.006>.
- (15) Pirrung, M. C. Synthetic Access to Cannabidiol and Analogs as Active Pharmaceutical Ingredients. *Journal of Medicinal Chemistry*. American Chemical Society November 12, 2020, pp 12131–12136. <https://doi.org/10.1021/acs.jmedchem.0c00095>.
- (16) Anand, R.; Cham, P. S.; Gannedi, V.; Sharma, S.; Kumar, M.; Singh, R.; Vishwakarma, R. A.; Singh, P. P. Stereoselective Synthesis of Nonpsychotic Natural Cannabidiol and Its Unnatural/Terpenyl/Tail-Modified Analogues. *J Org Chem* **2022**, *87* (7), 4489–4498. <https://doi.org/10.1021/acs.joc.1c02571>.
- (17) Grimm, J. A. A.; Zhou, H.; Properzi, R.; Leutzsch, M.; Bistoni, G.; Nienhaus, J.; List, B. Catalytic Asymmetric Synthesis of Cannabinoids and Menthol from Neral. *Nature* **2023**, *615* (7953), 634–639. <https://doi.org/10.1038/s41586-023-05747-9>.
- (18) Maiocchi, A.; Barbieri, J.; Fasano, V.; Passarella, D. Stereoselective Synthetic Strategies to (-)-Cannabidiol. *ChemistrySelect*. John Wiley and Sons Inc July 27, 2022. <https://doi.org/10.1002/slct.202202400>.
- (19) Baek, S.-H.; Srebnik, M.; Mechoulam, R. Boron Trifluoride Etherate on Alimina - a Modified Lewis Acid Reagent. *Tetrahedron Lett* **1985**, *26* (8), 1083–1086. [https://doi.org/10.1016/S0040-4039\(00\)98518-6](https://doi.org/10.1016/S0040-4039(00)98518-6).
- (20) Gaoni, Y.; Mechoulam, R. Hashish—VII: The Isomerization of Cannabidiol to Tetrahydrocannabinols. *Tetrahedron* **1966**, *22* (4), 1481–1488. [https://doi.org/10.1016/S0040-4020\(01\)99446-3](https://doi.org/10.1016/S0040-4020(01)99446-3).
- (21) Petrzilka, T.; Haefliger, W.; Sikemeier, C. Synthese von Haschisch-Inhaltsstoffen. 4. Mitteilung. *Helv Chim Acta* **1969**, *52* (4), 1102–1134. <https://doi.org/10.1002/hlca.19690520427>.
- (22) Bloemendal, V. R. L. J.; Spierenburg, B.; Boltje, T. J.; van Hest, J. C. M.; Rutjes, F. P. J. T. One-Flow Synthesis of Tetrahydrocannabinol and Cannabidiol Using Homo- and Heterogeneous Lewis Acids. *J Flow Chem* **2021**, *11* (2), 99–105. <https://doi.org/10.1007/s41981-020-00133-2>.
- (23) Crombie, L.; L. Crombie, W. M. Cannabinoid Bis-Homologues: Miniaturised Synthesis and GLC Study. *Phytochemistry* **1975**, *14* (1), 213–220. [https://doi.org/10.1016/0031-9422\(75\)85042-4](https://doi.org/10.1016/0031-9422(75)85042-4).
- (24) Appendino, G.; Gibbons, S.; Giana, A.; Pagani, A.; Grassi, G.; Stavri, M.; Smith, E.; Rahman, M. M. Antibacterial Cannabinoids from Cannabis Sativa: A Structure–Activity Study. *J Nat Prod* **2008**, *71* (8), 1427–1430. <https://doi.org/10.1021/mp8002673>.
- (25) Nguyen, G. N.; Jordan, E. N.; Kayser, O. Synthetic Strategies for Rare Cannabinoids Derived from Cannabis Sativa. *J Nat Prod* **2022**, *85* (6), 1555–1568. <https://doi.org/10.1021/acs.jnatprod.2c00155>.
- (26) Kulkarni, P. Methane Sulphonic Acid Is Green Catalyst in Organic Synthesis. *Oriental Journal of Chemistry* **2015**, *31* (1), 447–451. <https://doi.org/10.13005/ojc/310154>.
- (27) Crombie, L.; Crombie, W. M. L.; Firth, D. F. Terpenylations Using (R)-(-)- α -Phellandrene. Synthesis of the (3S,4R)-8,9-Dihydro-*o*- and -*p*-Cannabinoids, Their Iso-THC's, and the Natural Dihydrochalcone (3S,4R)-(+)-Linderatin. *J. Chem. Soc., Perkin Trans. I* **1988**, No. 5, 1251–1253. <https://doi.org/10.1039/P19880001251>.
- (28) Crombie, L.; Crombie, W. M. L.; Jamieson, S. V.; Palmer, C. J. Acid-Catalysed Terpenylations of Olivetol in the Synthesis of Cannabinoids. *J Chem Soc Perkin I* **1988**, No. 5, 1243. <https://doi.org/10.1039/p19880001243>.
- (29) Razdan, R. K.; Dalzell, H. C.; Handrick, G. R. Hashish. X. Simple One-Step Synthesis of (-)- Δ^9 -Tetrahydrocannabinol (THC) from *p*-Mentha-2,8-Dien-1-Ol and Olivetol. *J Am Chem Soc* **1974**, *96* (18), 5860–5865. <https://doi.org/10.1021/ja00825a026>.
- (30) Iwata, T.; Kawano, R.; Fukami, T.; Shindo, M. Retro-Friedel-Crafts-Type Acidic Ring-Opening of Triptycenes: A New Synthetic Approach to Acenes. *Chemistry - A European Journal* **2022**, *28* (12). <https://doi.org/10.1002/chem.202104160>.
- (31) Neese, F. The ORCA Program System. *Wiley Interdiscip Rev Comput Mol Sci* **2012**, *2* (1), 73–78.
- (32) Neese, F. Software Update: The ORCA Program System, Version 4.0. *Wiley Interdiscip Rev Comput Mol Sci* **2018**, *8* (1), e1327.
- (33) Neese, F.; Wennmohs, F.; Becker, U.; Riplinger, C. The ORCA Quantum Chemistry Program Package. *J Chem Phys* **2020**, *152* (22), 224108.

(34) Neese, F. Software Update: The ORCA Program System—Version 5.0. *WIREs Computational Molecular Science* **2022**, *12* (5), e1606.

(35) Grimme, S.; Hansen, A.; Ehlert, S.; Mewes, J.-M. R2SCAN-3c: A “Swiss Army Knife” Composite Electronic-Structure Method. *J Chem Phys* **2021**, *154* (6), 064103.

(36) Hobza, P. Stacking Interactions. *Physical Chemistry Chemical Physics*. 2008, pp 2581–2583. <https://doi.org/10.1039/b805489b>.

Table of Contents Graphic

